Self-organized waves in annular rf weakly magnetized dusty plasmas

Jeng-Mei Liu and Lin I
Department of Physics and Center for Complex System, National Central University, Chung-Li 32054, Taiwan, Republic of China
(Received 3 November 1999)

Self-organized waves and the associated dust particle motion are studied experimentally in a low-pressure annular rf weakly magnetized dusty discharge system. Low-frequency drift waves with strong modulation on plasma density and dark space (sheath) width, traveling azimuthally with mode number $m=1$, are self-excited. Period-n and quasiperiodic states are also observed at higher rf power. Dust particles in the liquid state show collective elliptical cyclic motion in the low-frequency ionization-drift wave but respond only weakly to waves with frequencies above 50 Hz. When dust is added to a dust-free magnetized discharge in which there exists an ionization drift wave at 20 KHz, the wave amplitude is reduced and the frequency is down shifted.

PACS number(s): 52.40.Hf, 52.35.Kt, 82.40.Bj

Dusty plasmas widely exist in various places from astroplasma to laboratory plasma systems [1,2]. Typically, a suspended micrometer dust particle in the background gaseous plasma with a few eV electron temperature can be charged up to 10^4 electrons. In addition to the strong dust-dust Coulomb coupling which leads to interesting dust Coulomb crystals exihibiting ordering at the microscopic scale [3–5], the massive dust particles are also strongly coupled with the background plasma through Coulomb interaction and dust charging processes. It modifies the macroscopic high-frequency plasma waves which exist in dust-free plasmas [6], and generates new low-frequency dusty waves associated with slow collective dust motion [7–10]. In the past few years, waves in dusty plasma systems have been widely studied theoretically [6–10], but much less well studied experimentally for the weakly ionized laboratory systems where the unfrozen ionization process and the inhomogeneity caused by the system boundary play important roles. In this work, using a steady state low pressure annular rf glow discharge system, we investigate the self-organized waves over a broad frequency range (a few Hz to tens of KHz) and the associated microscopic dust particle motion.

The weakly ionized discharge system is a nonlinear open-dissipative system. It exhibits many universal nonlinear behaviors [11] such as self-organized waves [12,13] and localized structures [14,15] with strong variation in ionization degree. A steady state discharge can be maintained under the balance between the electron-ion pair generation through ionization, and the loss through recombination in the plasma or on the chamber wall [12,16]. The ionization rate dominated by the electron impact excitation increases with local electron density and temperature. The ionization process is similar to reactions in chemical systems [11]. It provides a source for electron-ion generation and enhances plasma density fluctuations. The coupling between the ionization process and different types of transports, such as diffusion and drift-type transport induced by the space charge field, the spatial inhomogeneity around the boundary, and magnetic field, leads to the dissipative ionization or ionization-drift-type waves associated with ion density fluctuations [17]. In our previous studies, the self-organized ionization-drift waves with tens to hundreds of KHz frequency, and the transition from order to spatiotemporal chaos, have been observed experimentally in a cylindrical symmetric weakly magnetized dust-free discharge [13].

The addition of dust particles to the above discharge systems introduces new degrees of freedom. For example, through charge exchange and Coulomb interaction with the background plasma [7,9], the motion of dust particles can affect the local electron density, and in turn the sheath (dark space) width and the space charge field [18,19]. It further affects dust motions. Low-frequency waves with time scale controlled by the large inertia of dust particles can be self-organized, if a proper feedback phase can be maintained. Although the high-frequency (KHz) drift waves cause little collective dust motion due to the large dust mass, the dust charging and Coulomb interaction can still modify the high-frequency mode through the modification of dielectric properties [6]. It is found in our experiment that new low-frequency (a few to a few tens of Hz) ionization-drift waves associated with dust particle motions are self-excited. Dust

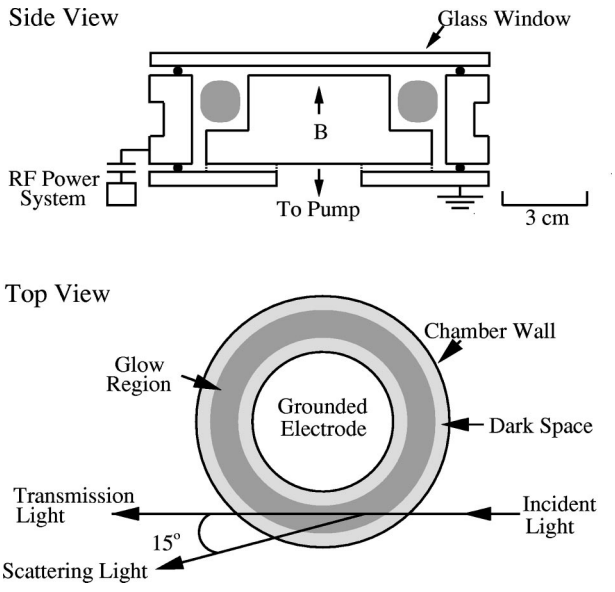

FIG. 1. The sketch of the system setup.

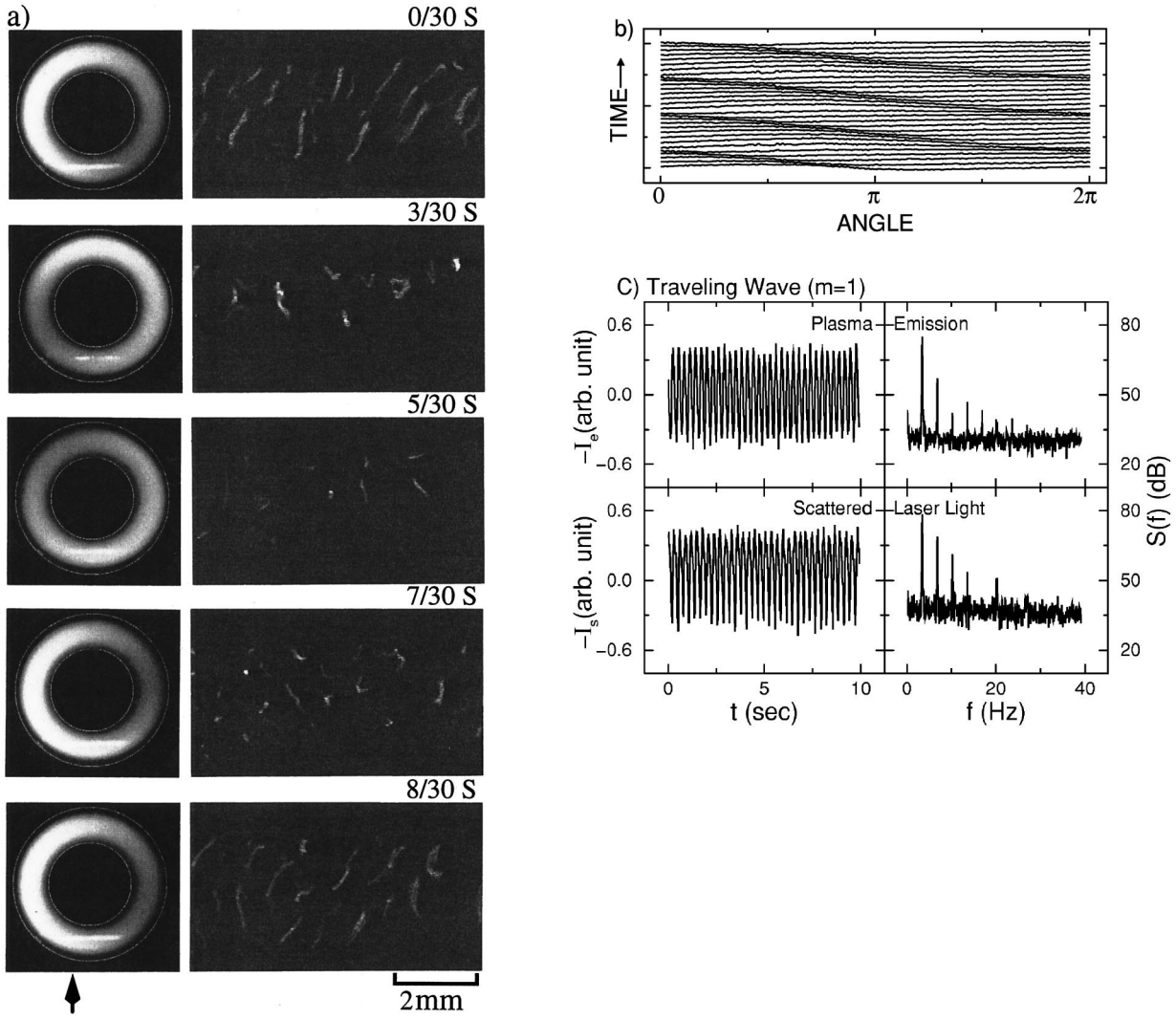

FIG. 2. (a) The sequential snapshots in one period of the 3.4-Hz self-organized traveling wave at 11 W and 65 G (left column), and magnified pictures with the associated particle motions (right column) at the laser illuminated point indicated by the arrow. The CCD camera is mounted on the top of the chamber. The exposure time is 20 msec for each frame. The bright circles in the left column indicate the edges of the two electrodes. (b) The space (toroidal angle)-time plot of the plasma emission intensity along a counterclockwise toroidal circle with $r=42$ mm. (c) The temporal evolutions and power spectra of the plasma emission and scattered laser light from a point measurement.

particles show collective elliptical cyclic motion in low-frequency waves, but have weak response to waves with frequency beyond 50 Hz. Changing the control prameter can tune the system to the period-n and quasiperiodic states. For the high-frequency ionization-drift wave (20 KHz) which exist in dust-free discharges, the wave amplitude is reduced and the frequency is down shifted when dust particles are added.

The experiment is conducted in an annular radio-frequency (rf) weakly ionized dusty discharge. It consists of a hollow outer electrode with 9-cm inner diameter and capacitively coupled to a 14-MHz rf power system, and a grounded center electrode with 5-cm diameter. Figure 1 shows the sketch of the system. With low pressure (30 mTorr) Ar gas and a uniform axial magnetic field ($B<100$ G), the steady state weakly ionized discharge can be divided into the annular glow region with $n_e \sim 3\times10^{10}$ cm^{-3} and the surrounding dark spaces (sheath) adjacent to the electrodes. The latter are about 5 mm thick and support large electron density gradient and a strong rf-induced dc electric field (~ 70 V/cm) outward from the poloidal center. SiO_2 particles (20–80 μm diameter) are generated through gas-phase reaction between O_2 and SiH_4 gases and confined in the annular Ar glow [3]. A 10-mW He-Ne laser with 2.5 mm expanded beam size is used to illuminate the dust particles. The intensity of the 15° forward scattered light, which is proportional to the local dust density, and the plasma emission intensity which is proportional to the local electron density, are simultaneously measured. For the low-frequency waves ($f<10$ Hz), the global emission distribution and the microscopic particle motions can be further monitored by the charge-coupled device (CCD) camera mounted on the top of the chamber, and another optical microscope/CCD system, respectively, with 30 Hz frame rate.

A self-organized low-frequency (5 Hz) standing wave associated with dust particle motion is observed (not shown) at

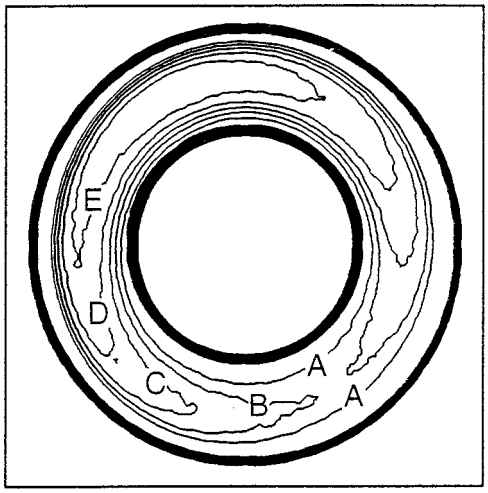

FIG. 3. The emission intensity contours of a typical snapshots image of the traveling wave. The concentric thick circles indicate the edges of the inner and outer electrodes. The intensity level differences between two adjacent contour lines are the same from A to E.

10 W rf power and 65 G. It bifurcates to a clockwise (left handed with respect to the upward B field) traveling wave at 11 W. The left column of Fig. 2(a) shows the sequential snapshot images of the plasma emission taken by the CCD camera in one cycle of the 3.4-Hz long wavelength (mode number $m=1$) traveling wave. The bright horizontal line with varying intensity corresponds to the scattered laser light under the variation of dust density along the laser path. The right column shows the magnified pictures with corresponding particle trajectories illuminated by the laser light at the position indicated by the arrow. Figure 2(b) shows the spatiotemporal evolution of the emission intensity taken along a toroidal circle with radius $r=42$ mm. The time evolutions and the power spectra of the intensities of the emission and the scattered light from the point measurement are shown in Fig. 2(c).

The discharge has a rotational symmetry before the onset of the wave. The glow region floats positively with respect to the surrounding wall due to the larger electron loss than ions. Increasing rf power can increase electron density and decrease the dark space width. The negatively charged dust particles are confined in the annular glow region by the surrounding dark space which supports a strong outward electric field. The outward ion flow pushes the particles with larger diameter closer to the glow-dark space boundary. The onset of the 3.4-Hz low-frequency traveling wave modulates the annular glow and the surrounding dark spaces. Figure 3 shows the snapshot of the emission intensity contour of a typical wave image. The intensity is roughly proportional to the electron density. It changes drastically in the dark space region. The dimmer (narrower) glow region (the 5 o'clock region in Fig. 3) is accompanied by the wider dark spaces. Because of the lower outward ion flow, dust particles are moved inward (poloidally) while the dimmer region comes by. The brighter glow region also floats more positively with respect to the dimmer glow region due to the higher space charge. Namely, the space charge field points out roughly normal to the glow intensity contour. There is an azimuthal electric field in the region between the brighter and dimmer glows. The varying electric fields associated with the traveling wave consequently induce horizontal and vertical cyclic collective particle motion. For example, the particles mainly travel horizontally in the first and last pictures of Fig. 2(a) but vertically in the rest pictures. There is a finite phase lag caused by the inertia of the massive dust particles. The observed particles (80 μm diameter) in Fig. 2(a) are located near the dark spaces in front of the bottom and the vertical surfaces of the inner electrode. They are hardly observed while moving upward out of the illuminated region [see the center images in Fig. 2(a)], when the dark space near the bottom electrode surface becomes wider. The particle motion induced by the varying electric field in the dark spaces can also be evidenced by the point measurement of the scattered laser light (the dust has a nonuniform radial density distribution). The oscillation of the scattered light intensity is about $90°$ phase lag in the emission intensity oscillation.

The dust particles gain high collective energy (as high as 4.2 MeV for a dust particle) from the particle-wave interaction. A simple estimation of 10-V potential variation in the dark spaces gives the result of about 4.2×10^{5} electrons per dust particle. Consequently, 4.9-Hz dust plasma frequency under 10^{3}-cm^{-3} dust density and 5.4×10^{-10}-Kg dust mass can be obtained. This is higher than the 3.4-Hz wave frequency. Therefore the dusts can response to the wave motion. The highest particle velocity is about 5 cm/sec but the wave velocity is about 70 cm/sec. Namely, the weak azimuthal electric field associated with the traveling wave cannot drive particles to the wave velocity and trap particles. It only modulates particle motion. The particles are in the liquid state with short range correlation and low random energy.

Besides the spontaneous breaking of the rotational symmetry for generating the standing and traveling waves, this highly complicated system also exhibits some other universal behaviors of the typical nonlinear extended systems [11]. For example, slightly increasing rf power makes the low-frequency mode bifurcate to period-n tupling modes. Figure 4(a) shows the behaviors of the plasma emission and the scattered laser light of a typical period-5 mode at 11.1-W rf power and 65 G. Another quasiperiodic route to chaos is found while rf power increases at $B=54$ G. The power spectrum in Fig. 4(b) shows the nonlinear coupling between the high (46 Hz) and the low (6 Hz) frequency bands at 35 W and 54 G. Note that, unlike the case of the low-frequency period-5 mode, the scattered light signal is more chaotic than electron density fluctuations under the 46-Hz oscillation. Dust particles are too heavy to respond to the high-frequency oscillation. They participate in the low-frequency (6 Hz) mode which is also nonlinearly coupled with the high-frequency mode. Its chaotic spectrum has a large continuous low-frequency noise background.

The system also supports self-organized KHz fluctuations in which particles show no collective motions. The high-frequency ionization-drift wave observed in other similar cylindrical dust-free magnetodischarge system [13] can be recovered at higher rf power and higher magnetic field. Figure 5(a) shows the temporal evolution of the point measurement of the plasma emission intensity and its power spectrum at 11 W and 72 G of a 20-KHz ionization-drift wave before

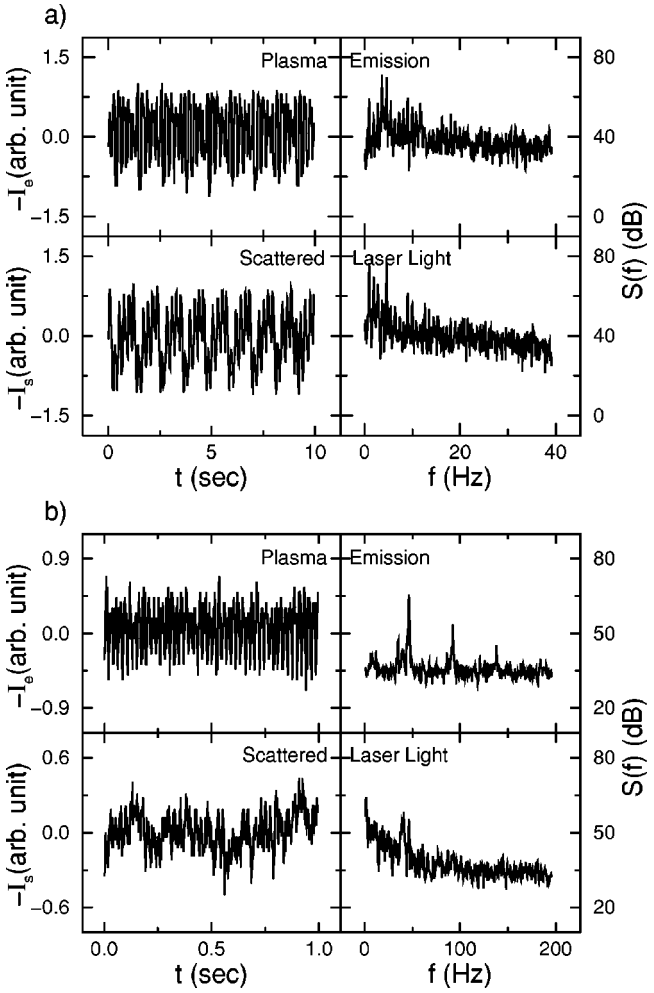

FIG. 4. The temporal evolutions and power spectra of the plasma emission and scattered laser light of the (a) period 5 at 11.1 W and 65 G, and the (b) quasiperiodic modes at 35 W and 54 G, respectively.

adding dust. The addition of dust particles increases the threshold rf power for generating this mode. Figure 5(b) shows that increasing rf power to 20 W cannot even fully recover the oscillation amplitude. The frequency is also down shifted to 16 KHz. The dust particles remain in the liquid state and their motions are not affected by the waves. Dust particles mainly drain electrons and ions (reducing the ionization degree), and change the plasma distribution. They modify the dielectric response and make the system more dissipative.

Basically, this system is an open-dissipative system driven by strong radial inhomogeneity and the external rf power source. The ionization degree is less than 1% and is not frozen. The low-frequency instability is a consequence of the interplay between the ionization-drift wave and the cyclic oscillation of dust particles in the liquid state. In the wave mode, the diffusion and drift processes can change the plasma density. The azimuthal rf power distribution is also spontaneously modulated due to the modulation of the local electron density which changes the local impedence and, in turn, the plasma density through ionization. It forms a nonuniform energy source to compensate the dissipation processes. The brighter glow region with a higher electron density is surrounded by a thinner dark space than the dimmer glow region. The former drains more rf power and sustains higher plasma density through the higher ionization rate. It also has larger positive space charges due to the larger loss rate difference between electrons and ions, and floats more positively with respect to the surrounding wall. The ambipolar diffusion and $E\times B$ drift under the strong inhomogeneity around the boundary provide spatial coupling and lead to the drift wave. The varying space charge fields and ion flows associated with the modulations of the background plasma density and dark space sheath modulate the dust motion. The motion of the dust particles further modulates the local plasma density, potential, and dark space width. It forms a feedback channel through the dust charging and electron repelling processes [9,18]. For example, the overshooting of the dust particles into the dark space region due to the expansion of the glow region can sink or expel electrons, and decrease the local ionization rate. It causes the expansion of the dark space (shrinking of the glow width) with a weaker outward ion flow, and drives the dust particles backward. The plasma fluctuation resonating with the cyclic dust motion can be spontaneously sustained. The temporal scale of oscillation and the feedback phase is determined by the slow dust dynamics. Note that our waves are different from the compressional dust lattice wave externally excited by an ac electric field for a cyrstal state [20], the highly nonlinear *great void* and *filamentary modes* in a magnetic field-free dusty-plasma system [21], and the short wavelength mode (<1 cm) in a revised dusty Q machine [22].

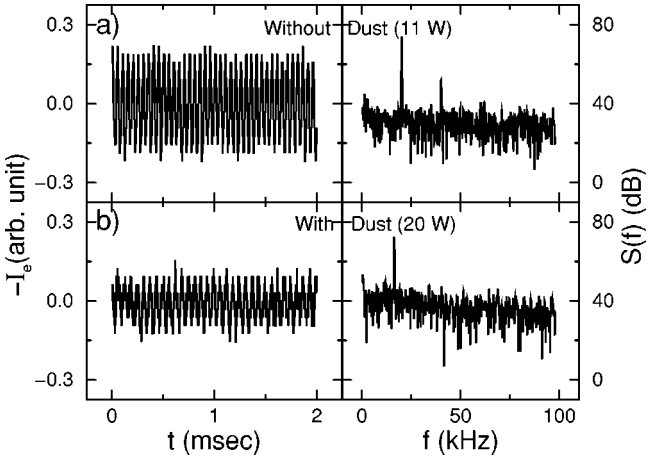

FIG. 5. The temporal evolutions and power spectra of the plasma emission intensity of the high-frequency drift mode without and with dust particles, respectively, at 72 G.

In conclusion, self-organized waves and the associated particle motion are observed in our weakly ionized and weakly magnetized dusty discharge. Dust particles are confined in the annular glow by the surrounding dark spaces. Low-frequency ionization-drift instabilities are strongly coupled with the varying electric fields in dark spaces and the induced cyclic elliptical dust particle motion. The oscillation amplitude of the dust motion drastically decreases with a frequency above a few tens of Hz. Their motions are frozen at tens of KHz. Dust particles drain electrons, modify dielectric properties, and attenuate the drift-type high-

frequency waves. From the nonlinear dynamics point of view, the generation of self-organized standing and traveling waves through the spontaneous breaking of the rotational symmetry, and the observation of the period-*n* and the quasiperiodic states manifest that, for such a complicated system, the universal dynamical behaviors are still followed as in many other different extended chemical systems.

This work is supported by the National Science Council of the Republic of China under Contract No. NSC-89-2112-M008-002.

[1] C. K. Goertz, Rev. Geophys. **27**, 271 (1989).
[2] D. A. Mendis and M. Rosenberg, Annu. Rev. Astron. Astrophys. **32**, 419 (1994).
[3] J. H. Chu and Lin I, Phys. Rev. Lett. **72**, 4009 (1994).
[4] Y. Hayshi and K. Tachibana, Jpn. J. Appl. Phys., Part 1 **33**, 804 (1994).
[5] H. Thomas *et al.*, Phys. Rev. Lett. **73**, 652 (1994).
[6] See, e.g., S. V. Vladimirov, Phys. Rev. E **50**, 1422 (1994); J. X. Ma and M. Y. Yu, *ibid.* **50**, R2431 (1994); A. Barkan, N. D'Angelo, and R. L. Merlino, Planet. Space Sci. **43**, 905 (1995); F. Li, *et al.*, *ibid.* **42**, 401 (1994).
[7] M. R. Jana, A. Sen, and P. K. Kaw, Phys. Scr. **51**, 385 (1995).
[8] N. N. Rao, P. K. Shukla, and M. Y. Yu, Planet. Space Sci. **38**, 543 (1990).
[9] M. R. Jana, A. Sen, and P. K. Kaw, Phys. Rev. E **48**, 3930 (1993); P. K. Kaw and R. Singh, Phys. Rev. Lett. **79**, 423 (1997).
[10] N. D'Angelo, Planet. Space Sci. **38**, 1143 (1990).
[11] M. C. Cross and P. C. Hohenberg, Rev. Mod. Phys. **65**, 851 (1993).
[12] Y. P. Raizer, *Gas Discharge Physics* (Springer, Berlin, 1987).
[13] J. H. Chu and Lin I, Phys. Rev. A **39**, 233 (1989); Lin I and J. M. Liu, *ibid.* **46**, R733 (1992); Phys. Rev. Lett. **74**, 3161 (1995).
[14] E. Ammelt, D. Schweng, and H.-G. Purwins, Phys. Lett. A **179**, 348 (1993); I. Muller, E. A. Ammelt, and H.-G. Purwins. Phys. Rev. Lett. **82**, 3428 (1999).
[15] C. Y. Liu and Lin I, Phys. Rev. E **57**, 3379 (1998).
[16] B. Chapman, *Glow Discharge Process* (Wiley, New York, 1980).
[17] S. V. Vladimirov and Lin I, J. Plasma Phys. **60**, 581 (1998).
[18] J. X. Ma and M. Y. Yu, Phys. Plasmas **2**, 1343 (1995).
[19] S. J. Choi, *et al.*, Appl. Phys. Lett. **59**, 3102 (1991).
[20] J. B. Pieper and J. Goree, Phys. Rev. Lett. **77**, 3137 (1996).
[21] G. Praburam and J. Goree, Phys. Plasmas **3**, 1212 (1996).
[22] A. Barkan *et al.*, Phys. Plasmas **2**, 3563 (1995).